

Thermodynamic Properties of Metal Amides Determined by Ammonia Pressure-Composition Isotherms

Satoshi Hino^a, Takayuki Ichikawa^{a,b*}, Yoshitsugu Kojima^{a,b}

^aGraduate School of Advanced Sciences of Matter, Hiroshima University, 1-3-1 Kagamiyama, Higashi-Hiroshima 739-8530, Japan

^bInstitute for Advanced Materials Research, Hiroshima University, 1-3-1 Kagamiyama, Higashi-Hiroshima 739-8530, Japan

*Corresponding author. Tel.: +81 82 424 5744; fax: +81 82 424 5744.

E-mail address: tichi@hiroshima-u.ac.jp (T. Ichikawa).

Abstract

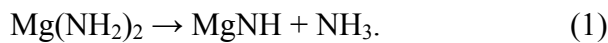
Thermodynamic properties of $\text{Mg}(\text{NH}_2)_2$ and LiNH_2 were investigated by measurements of NH_3 pressure-composition isotherms (PCI). Van't Hoff plot of plateau pressures of PCI for decomposition of $\text{Mg}(\text{NH}_2)_2$ indicated the standard enthalpy and entropy change of the reactions were $\Delta H^\circ = (120 \pm 11) \text{ kJ}\cdot\text{mol}^{-1}$ (per unit amount of NH_3) and $\Delta S^\circ = (182 \pm 19) \text{ J}\cdot\text{mol}^{-1}\cdot\text{K}^{-1}$ for the reaction: $\text{Mg}(\text{NH}_2)_2 \rightarrow \text{MgNH} + \text{NH}_3$, and $\Delta H^\circ = 112 \text{ kJ}\cdot\text{mol}^{-1}$ and $\Delta S^\circ = 157 \text{ J}\cdot\text{mol}^{-1}\cdot\text{K}^{-1}$ for the reaction: $\text{MgNH} \rightarrow (1/3)\text{Mg}_3\text{N}_2 + (1/3)\text{NH}_3$. PCI measurements for formation of LiNH_2 were carried out, and temperature dependence of plateau pressures indicated $\Delta H^\circ = (-108 \pm 15) \text{ kJ}\cdot\text{mol}^{-1}$ and $\Delta S^\circ = (-143 \pm 25) \text{ J}\cdot\text{mol}^{-1}\cdot\text{K}^{-1}$ for the reaction: $\text{Li}_2\text{NH} + \text{NH}_3 \rightarrow 2\text{LiNH}_2$.

Keywords: Hydrogen storage materials; Pressure-composition isotherms; Gas-solid reactions; van't Hoff plot; Heat of formation

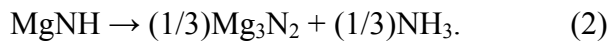
1. Introduction

Thermodynamic properties of metal amides were estimated from ammonia NH_3 Pressure-Composition (p - C) isotherms (PCI) for decomposition and formation of metal amides. Metal amides react with metal hydrides to desorb hydrogen and these reactions have been paid attention as new hydrogen storage systems since Chen et al.'s report [1]. Hydrogen desorbed from these compounds contaminated by a small amount of NH_3 originated from decomposition of the amides themselves, which would be a problem for an application of these systems [2, 3]. Therefore, thermodynamic properties of the metal amides are important, and the thermodynamics of metal-N-H system should be discussed by taking account of the thermodynamics of elementary reactions.

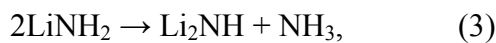
The chemistry of the alkali and alkaline earth metal amides has been the subject of a large number of investigations [4, 5]. Thermal decomposition properties of metal amides under inert gas flow (or in vacuum) have been investigated. Magnesium amide $\text{Mg}(\text{NH}_2)_2$ decomposes to magnesium imide MgNH and NH_3 by heating to $T = 573 - 673$ K through the following reaction [6] :



Then, magnesium imide decomposes into magnesium nitride Mg_3N_2 with NH_3 release at more than $T = 623$ K as follows:



Lithium amide LiNH_2 decomposes to lithium imide Li_2NH and NH_3 at temperatures of $573 - 673$ K [7, 8] :



and imide decomposes into lithium nitride at higher temperatures. In addition, the enthalpies of formation of LiNH_2 and Li_2NH have been reported from the measurements of the heat of dissolution [9].

Thermodynamic properties (e.g. standard enthalpy or entropy change of reaction, ΔH° and ΔS°) of metal-hydrogen systems have been investigated by measuring p - C isotherms [10]. The p - C isotherms of decomposition (and formation) of LiNH_2 to (from) Li_2NH at $T = 573$ K and $T = 673$ K have been reported in 1951 [8]. Liu et al. [11] has reported the results of p - C isotherms of decompositions of LiNH_2 and $\text{Mg}(\text{NH}_2)_2$. These measurements were performed above the melting point of LiNH_2 ($T = 653$ K) and $\text{Mg}(\text{NH}_2)_2$ ($T = 633$ K). LiNH_2 volatilizes around $T = 673$ K and may be sublimed under pressure in an ammonia atmosphere [12], which may prevent accurate determination of equilibrium pressures. In the present work, all p - C isotherms were carried out below the melting point of the metal amides. Temperature dependences of plateau pressures p were measured to determine ΔH° and ΔS° of the reactions for the decomposition or

formation of the metal amides from van't Hoff equation ($\ln (p/p^0) = -\Delta H^0/RT + \Delta S^0/R$, where p^0 is standard pressure 0.1 MPa, R the gas constant and T absolute temperature).

Decomposition reaction of ammonia to nitrogen and hydrogen ($2\text{NH}_3 \rightarrow \text{N}_2 + 3\text{H}_2$) should be considered during the NH_3 PCI measurements. In the viewpoint of thermodynamics, equilibrium NH_3 conversion to N_2 and H_2 is >90% above $T = 573$ K under normal pressure [13]. Therefore, amounts of generated H_2 were measured by gas chromatography (GC), and net NH_3 pressures were evaluated.

2. Experimental

$\text{Mg}(\text{NH}_2)_2$ was synthesized by reacting MgH_2 under gaseous NH_3 flow ($p = 0.5$ MPa, at a flow rate of $25 \text{ ml}\cdot\text{min}^{-1}$) at $T = 473$ K for 14 days ($\text{MgH}_2 + 2\text{NH}_3 \rightarrow \text{Mg}(\text{NH}_2)_2 + 2\text{H}_2$). LiNH_2 (Sigma-Aldrich Co., 95%) was heated up to $T = 723$ K under vacuum for 10 h to derive Li_2NH . Li_2NH was activated by ball-milling (Fritsch, P7) under Ar atmosphere for 2 h and was provided for PCI measurement of formation of LiNH_2 . All handling of chemicals took place in a glove box filled with purified Ar.

NH_3 p - C isotherms were measured using a Sieverts type apparatus. Prior to the sample measurement, blank p - C isotherms were measured, and as a result, the total pressure was found to increase slightly due to the NH_3 decomposition.

Desorption PCI: ~100 mg sample was loaded in a sample holder (10ml volume). The system was evacuated, and sufficient amount of NH_3 (5N) gas was introduced into the system. The sample cell was heated up to a measurement temperature with a heating rate of $5 \text{ K}\cdot\text{min}^{-1}$ and the temperature was held constant. Pressure change was monitored by a pressure transducer (GE Druck, PDCR-4000) and data acquisition system. After stabilizing the pressure (waiting time: 1-12 h), gas in the reservoir (61 or 14 ml volume) was introduced to a gas chromatograph (GC-14B, Shimadzu Corp.) to determine H_2 and N_2 amounts from GC peak intensities. Pure H_2 (7N) and N_2 (99.99995%) gases are used for calibration of the GC peak area and gas pressure. Net NH_3 equilibrium pressure and the amount of decomposed ammonia were estimated by subtracting H_2 and N_2 pressures from total pressure, as a result, one data point of PCI curve was derived. Stepwise decrease in NH_3 pressure followed by waiting for equilibrium and GC measurement were continued. In the case of waiting time exceeded 12 h, measurement went next step, because such slow pressure increase may be caused by NH_3 decomposition.

Absorption PCI: ~50 mg sample was loaded in the sample holder and the system was evacuated and then heated. The NH_3 gas was introduced to apply stepwise increase in the pressure. At each pressure, waiting time of 15 min was adopted to realize

the equilibrium state, because the absorption reaction showed fast kinetics. It was difficult to perform the GC measurement for the analysis of the gas composition, since equilibrium pressures were very low.

Powder X-ray diffraction (RINT-2500V, Rigaku, Cu-K α radiation) measurement was carried out at room temperature to identify phases before and after the PCI measurements.

3. Results and Discussion

The p - C isotherms of the decomposition of $\text{Mg}(\text{NH}_2)_2$ to MgNH were measured at lower temperatures than the melting point of $\text{Mg}(\text{NH}_2)_2$, i.e. $T = 633$ K. Total pressure gradually increased during the desorption measurement with a rate of $0.2 - 1 \text{ kPa}\cdot\text{h}^{-1}$, which may be caused by decomposition of NH_3 itself. Therefore, the GC measurement was carried out to subtract H_2 and N_2 contribution to the total pressure and actual NH_3 pressure was estimated. Fig. 1 shows NH_3 p - C isotherms of decomposition of $\text{Mg}(\text{NH}_2)_2$ at $T = (583, 603 \text{ and } 623)$ K. Plateau regions which corresponded to the decomposition of amide phase to imide phase appeared, and the plateau pressures, i.e., the values of the pressures at the midpoint of the plateau, are $p = (6.0, 15.6 \text{ and } 29.4)$ kPa at $T = (583, 603, 623)$ K, respectively. Plateau region of the decomposition of MgNH to Mg_3N_2 was not observed, therefore, the plateau pressure of the decomposition of imide to nitride phase may be too low at these temperatures. For the isotherms at temperatures of 623 and 583 K, the lengths of the plateau regions did not reach a theoretical value (25%). It could be caused by decrease in surface or bulk activity of a part of the powder sample by long time sintering. We suppose a small amount of deactivated powders have no significant effect for the plateau pressure. XRD profiles of the sample after desorption PCI measurement at $T = 603$ K are shown in Fig. 2(a), which shows the presence of MgNH phase after the PCI measurement.

Higher temperature was applied to measure p - C isotherms of decomposition of MgNH to Mg_3N_2 . Fig. 3 shows the PCI curves of the reaction (2) at $T = (663, 683 \text{ and } 693)$ K. The plateau regions which corresponded to the decomposition of imide phase to nitride phase appeared for the measurements at temperatures of 663 K and 683 K, and the values of the plateau pressures are $p = 8.0$ kPa at $T = 663$ K, $p = 14.9$ kPa at $T = 683$ K. After the desorption PCI measurement at $T = 693$ K, main phase was Mg_3N_2 in XRD profile as shown in Fig. 2(b).

The NH_3 desorption plateau pressures in van't Hoff plot ($\ln(p/p^0)$ vs. T^{-1}) are shown in Fig. 4(a,b). The slope of $\ln(p/p^0)$ and the intercept corresponds to ΔH^0 and ΔS^0 , respectively. The results are $\Delta H^0 = (120 \pm 11) \text{ kJ}\cdot\text{mol}^{-1}$ and $\Delta S^0 = (182 \pm 19)$

$\text{J}\cdot\text{mol}^{-1}\cdot\text{K}^{-1}$ for the reaction (1), and $\Delta H^{\circ} = 112 \text{ kJ}\cdot\text{mol}^{-1}$ and $\Delta S^{\circ} = 157 \text{ J}\cdot\text{mol}^{-1}\cdot\text{K}^{-1}$ for the reaction (2). Here, we define the unit as per mole amount of NH_3 for the reactions. Liu et al. [11] have reported much higher NH_3 equilibrium pressure ($p = \text{ca. } 200 \text{ kPa}$ at $T = 623 \text{ K}$) for the decomposition of $\text{Mg}(\text{NH}_2)_2$ to MgNH in the temperature range of $T = 613 - 643 \text{ K}$, and calculated smaller enthalpy change of NH_3 generation ($\Delta H_{\text{ref}}^{\circ} = 40.8 \text{ kJ}\cdot\text{mol}^{-1}$). Such high pressures could come from the decomposition of NH_3 to H_2 and N_2 , and van't Hoff plot of the total pressures could not show ΔH° of the decomposition of the amide. In our work, the partial pressures of H_2 and N_2 were calculated by the GC measurement.

Using ΔH° and ΔS° values above and literature values of the standard enthalpy $\Delta^{\text{f}}H^{\circ}$ of formation and standard entropy S° for Mg_3N_2 and NH_3 [14], one can derive $\Delta^{\text{f}}H^{\circ}$ and S° of $\text{Mg}(\text{NH}_2)_2$ and MgNH as shown in Table 1. Hu et al. [15] reported the standard enthalpy of formation of $\text{Mg}(\text{NH}_2)_2$ measured by differential scanning calorimetry (DSC) and dissolution calorimetry as -325 and $-351 \text{ kJ}\cdot\text{mol}^{-1}$, respectively. We suspect the contributions of gas phase NH_3 to the DSC signal (such as heat capacity and heat of evaporation) may not be sufficiently treated, while, the $\Delta^{\text{f}}H^{\circ}$ value measured from the heat of dissolution of $\text{Mg}(\text{NH}_2)_2$ is in reasonable agreement with our result.

The p - C isotherms of the formation of LiNH_2 from Li_2NH were measured at lower temperatures than the melting point of LiNH_2 , i.e. $T = 643 \text{ K}$. Fig. 5 shows NH_3 p - C isotherms of formation of LiNH_2 at $T = (583, 603 \text{ and } 623) \text{ K}$. The plateau regions which corresponded to the formation of amide phase from imide phase appeared, the plateau pressures are $p = (0.7, 1.2 \text{ and } 2.8) \text{ kPa}$ at $T = (583, 603 \text{ K and } 623) \text{ K}$, respectively. The isotherms ended around 80 % of NH_3 absorption, which could be caused by partial deactivation of the powder sample. XRD profiles of the samples before and after the absorption PCI measurement at $T = 583 \text{ K}$ are shown in Fig. 2(c, d), which indicated main phase is LiNH_2 after the PCI measurement.

The plateau pressures in van't Hoff plot ($\ln(p/p^{\circ})$ vs. T^{-1}) are shown in Fig. 4(c). Least-squares fit of the plot gives ΔH° and ΔS° . The results are $\Delta H^{\circ} = (108 \pm 15) \text{ kJ}\cdot\text{mol}^{-1}$ and $\Delta S^{\circ} = (143 \pm 25) \text{ J}\cdot\text{mol}^{-1}\cdot\text{K}^{-1}$. Liu et al. [11] have measured NH_3 equilibrium pressures for the decomposition of LiNH_2 in the temperature range of $T = 633 - 678 \text{ K}$, and calculated enthalpy change of NH_3 generation to be $43.4 \text{ kJ}\cdot\text{mol}^{-1}$. (They have described the unit as $\text{kJ}\cdot\text{mol}^{-1}$ per unit amount of LiNH_2 , however it should be $\text{kJ}\cdot\text{mol}^{-1}$ per unit amount of NH_3). This $\Delta H_{\text{ref}}^{\circ}$ value is about half of the value derived by the present work, and the values of equilibrium pressure are much higher than the extrapolated values of our work at high temperatures. The NH_3 decomposition could result in these high pressures, if they have measured the equilibrium pressure by directly

using a pressure transducer. If the NH_3 partial pressures have been calculated from ion concentrations in the gaseous phase, the high pressures could be caused by sublimed LiNH_2 . We also noted, above the melting point of the amides, ΔH° and ΔS° of the amide decomposition reactions would be smaller than those values measured below the melting point. Because $\Delta^f H^\circ$ and S° of solid phase should be smaller than those of liquid phase for the metal amides. Therefore, our measurements were carried out below the melting point of the amides. Using reported $\Delta^f H^\circ$ values (LiNH_2 : $-186.3 \text{ kJ}\cdot\text{mol}^{-1}$) in our previous work [16] and in the literature [14] (NH_3 : $-45.9 \text{ kJ}\cdot\text{mol}^{-1}$), one obtains $\Delta^f H^\circ$ value of Li_2NH as $\Delta^f H^\circ (\text{Li}_2\text{NH}) = (-219 \pm 24) \text{ kJ}\cdot\text{mol}^{-1}$. This value is in good agreement with the literature [9] ($\Delta^f H^\circ_{\text{ref}} (\text{Li}_2\text{NH}) = -220 \text{ kJ}\cdot\text{mol}^{-1}$).

4. Conclusions

NH_3 pressure-composition isotherms for decomposition of $\text{Mg}(\text{NH}_2)_2$ and formation of LiNH_2 were measured at lower temperatures than melting points of the metal amides. During the decomposition isotherms of $\text{Mg}(\text{NH}_2)_2$, H_2 and N_2 generation due to NH_3 decomposition was observed by gas chromatography. Temperature dependences of NH_3 plateau pressures gave ΔH° and ΔS° values for the decomposition or formation of the metal amides. The results are $\Delta H^\circ = (120 \pm 11) \text{ kJ}\cdot\text{mol}^{-1}$ and $\Delta S^\circ = (182 \pm 19) \text{ J}\cdot\text{mol}^{-1}\cdot\text{K}^{-1}$ for the reaction $\text{Mg}(\text{NH}_2)_2 \rightarrow \text{MgNH} + \text{NH}_3$, $\Delta H^\circ = 112 \text{ kJ}\cdot\text{mol}^{-1}$ and $\Delta S^\circ = 157 \text{ J}\cdot\text{mol}^{-1}\cdot\text{K}^{-1}$ for the reaction $\text{MgNH} \rightarrow (1/3)\text{Mg}_3\text{N}_2 + (1/3)\text{NH}_3$, and, $\Delta H^\circ = (-108 \pm 15) \text{ kJ}\cdot\text{mol}^{-1}$ and $\Delta S^\circ = (-143 \pm 25) \text{ J}\cdot\text{mol}^{-1}\cdot\text{K}^{-1}$ for the reaction $\text{Li}_2\text{NH} + \text{NH}_3 \rightarrow \text{LiNH}_2$. The standard enthalpy $\Delta^f H^\circ$ of formation and standard entropy S° were derived as follows: $\Delta^f H^\circ(\text{Mg}(\text{NH}_2)_2) = (-374 \pm 11) \text{ kJ}\cdot\text{mol}^{-1}$, $S^\circ(\text{Mg}(\text{NH}_2)_2) = (52 \pm 19) \text{ J}\cdot\text{mol}^{-1}\cdot\text{K}^{-1}$, $\Delta^f H^\circ(\text{MgNH}) = -208 \text{ kJ}\cdot\text{mol}^{-1}$, $S^\circ(\text{MgNH}) = 41 \text{ J}\cdot\text{mol}^{-1}\cdot\text{K}^{-1}$, $\Delta^f H^\circ(\text{Li}_2\text{NH}) = (-219 \pm 24) \text{ kJ}\cdot\text{mol}^{-1}$.

Acknowledgements

This work was partially supported by NEDO project ‘‘Advanced Fundamental Research on Hydrogen Storage Materials’’ in Japan, and Grant-in-Aid for JSPS (Japanese Society for the Promotion of Science) Fellows (no.188366). The authors are grateful to Dr. E. Akiba (National Institute of Advanced Industrial Science and Technology) for valuable suggestions.

References

- [1] P. Chen, Z. T. Xiong, J. Z. Luo, J. Y. Lin, K. L. Tan, *Nature* **420** (2002)

302-304.

- [2] W. Luo, K. Stewart, *J. Alloys Compd.* **440** (2007) 357-361.
- [3] S. Ikeda, N. Kuriyama, T. Kiyobayashi, *Int. J. Hydrogen Energy* **33** (2008) 6201-6204.
- [4] F. W. Bergstrom, W. C. Fernelius, *Chem. Rev.* **12** (1933) 43.
- [5] R. Juza, *Angew. Chem. internat. Edit.* **3** (1964) 471.
- [6] H. Y. Leng, T. Ichikawa, S. Hino, N. Hanada, S. Isobe, H. Fujii, *J. Power Sources* **156** (2006) 166-170.
- [7] O. Ruff, H. Goerges, *Chem. Ber.* **44** (1910) 502-506.
- [8] R. Juza, K. Opp, *Z. anorg. allg. Chem.* **266** (1951) 325-330.
- [9] A. Guntz, F. Benoit, *Ann. Chim.* [**9**] **20** (1923) 5-33.
- [10] G. Sandrock, *J. Alloys Compd.* **293** (1999) 877-888.
- [11] Y. F. Liu, J. J. Hu, G. T. Wu, Z. T. Xiong, P. Chen, *J. Phys. Chem. C* **112** (2008) 1293-1298.
- [12] A. W. Titherley, *J. Chem. Soc.* **65** (1894) 504-522.
- [13] S.-F. Yin, Q.-H. Zhang, B.-Q. Xu, W.-X. Zhu, C.-F. Ng, C.-T. Au, *J. Catal.* **224** (2004) 384-396.
- [14] M. W. Chase, Jr. (Ed.), *NIST-JANAF Thermochemical Tables, Fourth Edition*, *J. Phys. Chem. Ref. Data, Monograph 9*, (1998).
- [15] J. Hu, G. Wu, Y. Liu, Z. Xiong, P. Chen, K. Murata, K. Sakata, G. Wolf, *J. Phys. Chem. B* **110** (2006) 14688-14692.
- [16] S. Hino, T. Ichikawa, N. Ogita, M. Udagawa, Y. Kojima, *J. Appl. Phys.* **105** (2009) 023527-1 - 023527-3.

Figure legends

Table 1. Thermodynamic functions of reactions and compounds. The units are defined as per mole amount of NH_3 and each compounds for the reactions and compounds, respectively.

Fig.1 Pressure-composition isotherms for decomposition of $\text{Mg}(\text{NH}_2)_2$ at $T = 583 \text{ K}$ (\circ), $T = 603 \text{ K}$ (Δ), and $T = 623 \text{ K}$ (\square). The horizontal axis shows the percent of ammonia left to desorb, where $x\text{NH}_3$ desorbs through the following reaction: $\text{Mg}(\text{NH}_2)_2$ (100%) \rightarrow MgNH (25%) + $\text{NH}_3 \rightarrow (1/3)\text{Mg}_3\text{N}_2$ (0%) + $(4/3)\text{NH}_3$.

Fig.2 Powder X-ray diffraction profiles (intensities I in arbitrary units) before and after pressure-composition isotherms (PCI): (a) after decomposition PCI of $\text{Mg}(\text{NH}_2)_2$ at $T = 603 \text{ K}$, (b) after decomposition PCI of MgNH at $T = 693 \text{ K}$, (c) before and (d) after formation PCI of LiNH_2 at $T = 583 \text{ K}$. The peak positions of the typical reflections in the ICDD powder diffraction files are included for comparison: $\text{Mg}(\text{NH}_2)_2$ (#72-0786), MgNH (#23-0391), Mg_3N_2 (#35-0778), Li_2NH (#75-0050), LiNH_2 (#71-1616).

Fig.3 Pressure-composition isotherms for decomposition of MgNH at $T = 663 \text{ K}$ (\circ), $T = 683 \text{ K}$ (Δ), and $T = 693 \text{ K}$ (\square). The horizontal axis shows the percent of ammonia left to desorb, where $x\text{NH}_3$ desorbs through the following reaction: $\text{Mg}(\text{NH}_2)_2$ (100%) \rightarrow MgNH (25%) + $\text{NH}_3 \rightarrow (1/3)\text{Mg}_3\text{N}_2$ (0%) + $(4/3)\text{NH}_3$.

Fig.4 Van't Hoff plot of plateau pressures for: (a) decomposition of $\text{Mg}(\text{NH}_2)_2$ to MgNH , (b) decomposition of MgNH to Mg_3N_2 , (c) formation of LiNH_2 from Li_2NH .

Fig.5 Pressure-composition isotherms for formation of LiNH_2 at $T = 583 \text{ K}$ (\circ), $T = 603 \text{ K}$ (Δ), and $T = 623 \text{ K}$ (\square). The horizontal axis shows the percent of absorbed ammonia ($x\text{NH}_3$) through the following reaction: Li_2NH (0%) + $\text{NH}_3 \rightarrow 2\text{LiNH}_2$ (100%).

Table 1. Thermodynamic functions of reactions and compounds. The units are defined as per mole amount of NH₃ and each compounds for the reactions and compounds, respectively.

reaction or compound	this work		lit.		ref.
	$\Delta H^{\circ} / \text{kJ}\cdot\text{mol}^{-1}$	$\Delta S^{\circ} / \text{J}\cdot\text{mol}^{-1}\cdot\text{K}^{-1}$	$\Delta H^{\circ} / \text{kJ}\cdot\text{mol}^{-1}$	$\Delta S^{\circ} / \text{J}\cdot\text{mol}^{-1}\cdot\text{K}^{-1}$	
$\text{Mg}(\text{NH}_2)_2 \rightarrow \text{MgNH} + \text{NH}_3$	120 ± 11	182 ± 19	40.8	70.6	[9]
$\text{MgNH} \rightarrow (1/3)\text{Mg}_3\text{N}_2 + (1/3)\text{NH}_3$	112	157			
$2\text{LiNH}_2 \rightarrow \text{Li}_2\text{NH} + \text{NH}_3$	108 ± 15	143 ± 25	43.4	71.5	[9]
	$\Delta^{\text{f}}H^{\circ} / \text{kJ}\cdot\text{mol}^{-1}$	$S^{\circ} / \text{J}\cdot\text{mol}^{-1}\cdot\text{K}^{-1}$	$\Delta^{\text{f}}H^{\circ} / \text{kJ}\cdot\text{mol}^{-1}$	$S^{\circ} / \text{J}\cdot\text{mol}^{-1}\cdot\text{K}^{-1}$	
Mg(NH ₂) ₂	-374 ± 11	52 ± 19	-325, -351		[13]
MgNH	-208	41			
Li ₂ NH	-219 ± 24		-220		[7]
NH ₃ (gas)			-45.9	192.77	[12]
Mg ₃ N ₂			-461.08	87.86	[12]
LiNH ₂			-186.3 ± 9.1		[14]

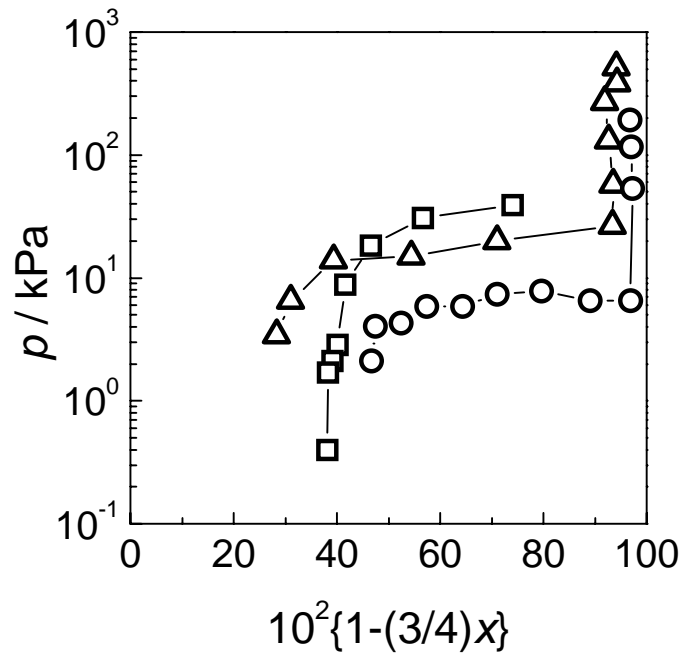


Fig.1 Pressure-composition isotherms for decomposition of $\text{Mg}(\text{NH}_2)_2$ at $T = 583 \text{ K}$ (\circ), $T = 603 \text{ K}$ (Δ), and $T = 623 \text{ K}$ (\square). The horizontal axis shows the percent of ammonia left to desorb, where $x\text{NH}_3$ desorbs through the following reaction: $\text{Mg}(\text{NH}_2)_2$ (100%) \rightarrow MgNH (25%) + NH_3 \rightarrow $(1/3)\text{Mg}_3\text{N}_2$ (0%) + $(4/3)\text{NH}_3$.

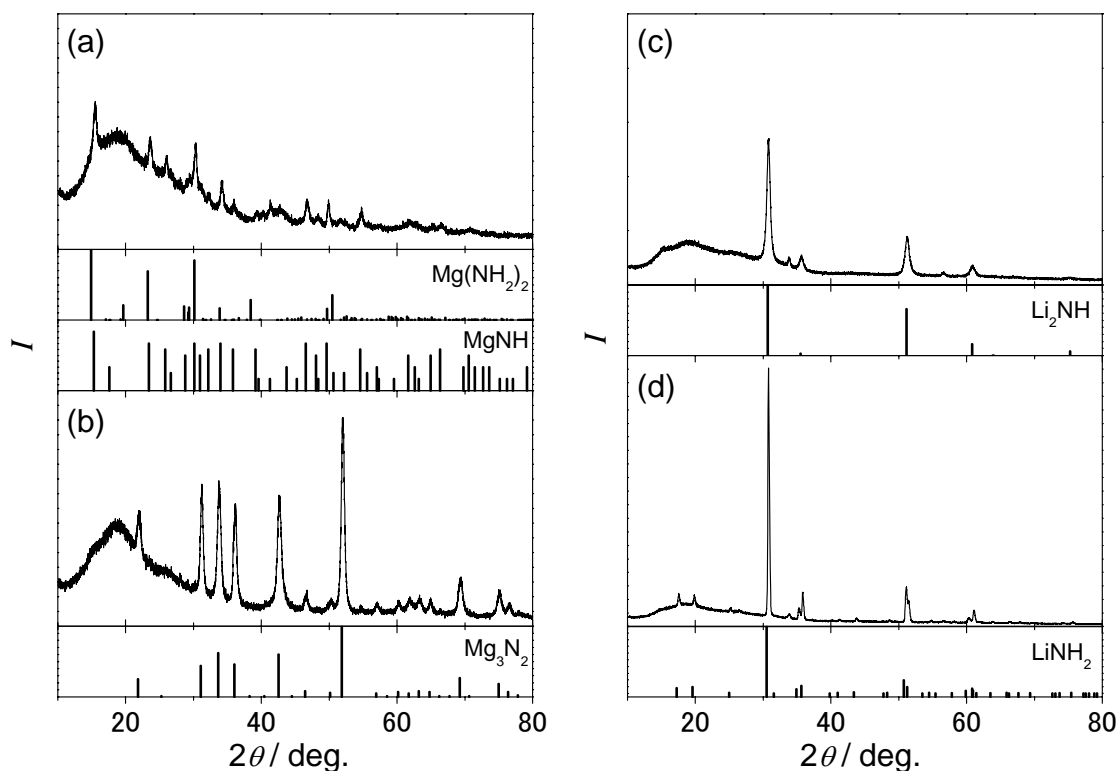


Fig.2 Powder X-ray diffraction profiles (intensities I in arbitrary units) before and after pressure-composition isotherms (PCI): (a) after decomposition PCI of $\text{Mg}(\text{NH}_2)_2$ at $T = 603$ K, (b) after decomposition PCI of MgNH at $T = 693$ K, (c) before and (d) after formation PCI of LiNH_2 at $T = 583$ K. The peak positions of the typical reflections in the ICDD powder diffraction files are included for comparison: $\text{Mg}(\text{NH}_2)_2$ (#72-0786), MgNH (#23-0391), Mg_3N_2 (#35-0778), Li_2NH (#75-0050), LiNH_2 (#71-1616).

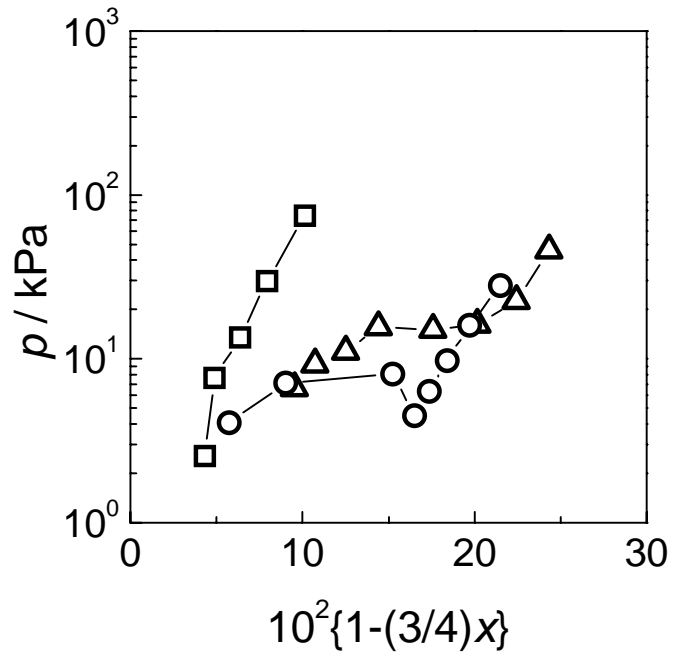


Fig.3 Pressure-composition isotherms for decomposition of MgNH at $T = 663$ K (○), $T = 683$ K (△), and $T = 693$ K (□). The horizontal axis shows the percent of ammonia left to desorb, where $x\text{NH}_3$ desorbs through the following reaction: $\text{Mg}(\text{NH}_2)_2$ (100%) \rightarrow MgNH (25%) + $\text{NH}_3 \rightarrow (1/3)\text{Mg}_3\text{N}_2$ (0%) + $(4/3)\text{NH}_3$.

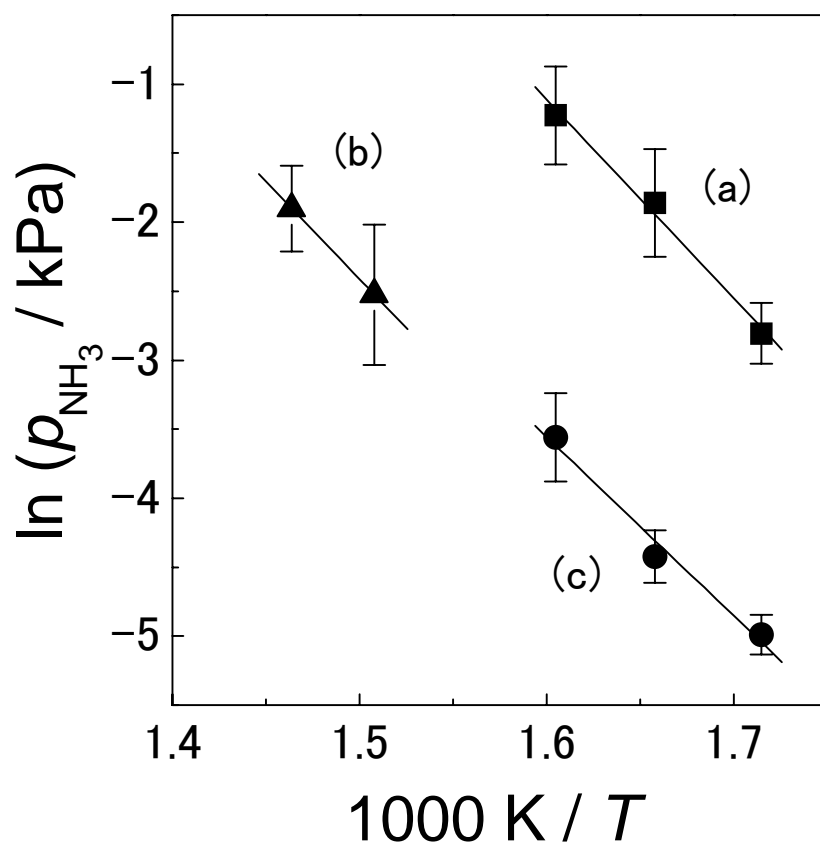


Fig.4 Van't Hoff plot of plateau pressures for: (a) decomposition of $\text{Mg}(\text{NH}_2)_2$ to MgNH , (b) decomposition of MgNH to Mg_3N_2 , (c) formation of LiNH_2 from Li_2NH .

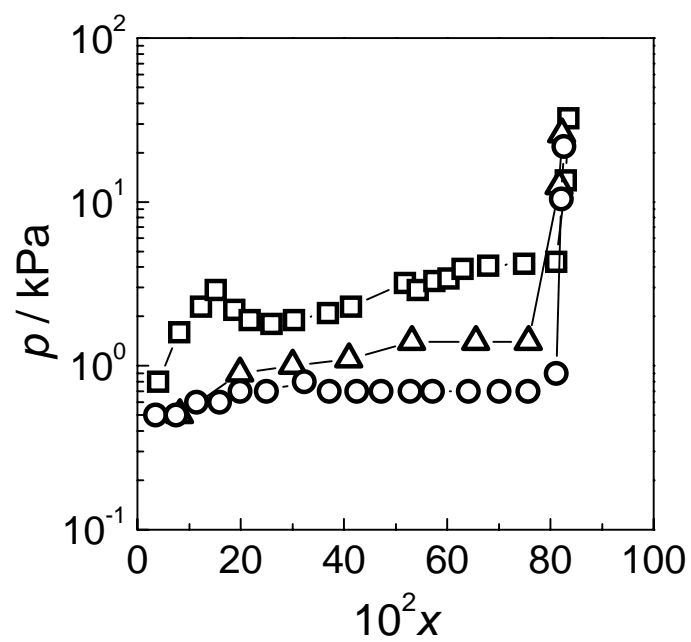


Fig.5 Pressure-composition isotherms for formation of LiNH_2 at $T = 583 \text{ K}$ (\circ), $T = 603 \text{ K}$ (Δ), and $T = 623 \text{ K}$ (\square). The horizontal axis shows the percent of absorbed ammonia ($x\text{NH}_3$) through the following reaction: Li_2NH (0%) + $\text{NH}_3 \rightarrow 2\text{LiNH}_2$ (100%).